1521-0111/12/8202-217–225$25.00
MOLECULAR PHARMACOLOGY
Vol. 82, No. 2
78824/3781658

Mol Pharmacol 82:217–225, 2012

The Guanine Nucleotide Exchange Factor Vav2 Is a Negative Regulator of Parathyroid Hormone Receptor/G_q Signaling[S]

Alexander Emami-Nemini, Antje Gohla, Henning Urlaub, Martin J. Lohse, and Christoph Klenk

Institute of Pharmacology and Toxicology (A.E.N., A.G., M.J.L., C.K.) and Rudolf Virchow Center (A.G., M.J.L.), University of Würzburg, Würzburg, Germany; Bioanalytical Mass Spectrometry Group, Max Planck Institute for Biophysical Chemistry, Göttingen, Germany (H.U.); and Department of Clinical Chemistry, University Medical Center Göttingen, Göttingen, Germany (H.U.)

Received March 19, 2012; accepted May 3, 2012

ABSTRACT

The parathyroid hormone receptor (PTHR) is a class B G protein-coupled receptor (GPCR) that mediates the endocrine and paracrine effects of parathyroid hormone and related peptides through the activation of phospholipase Cβ-, adenylyl cyclase-, mitogen-activated protein kinase-, and β-arrestin-initiated signaling pathways. It is currently not clear how specificity among these downstream signaling pathways is achieved. A possible mechanism involves adaptor proteins that affect receptor/effector coupling. In a proteomic screen with the PTHR C terminus, we identified vav2, a guanine nucleotide exchange factor (GEF) for Rho GTPases, as a PTHR-interacting protein. The core domains of vav2 bound to the intracellular domains of the PTHR independent of receptor activation. In addition, vav2 specifically interacted with activated Gα_q but not with Gα_s subunits, and it competed with PTHR for coupling to Gα_q. Consistent with its specific interaction with Gα_q, vav2 impaired G_q-mediated inositol phosphate generation but not G_s-mediated cAMP generation. This inhibition of G_q signaling was specific for PTHR signaling, compared with other G_q-coupled GPCRs. Moreover, the benefit for PTHR-mediated inositol phosphate generation in the absence of vav2 required the ezrin binding domain of Na^+/H^+-exchanger regulatory factor 1. Our results show that a RhoA GEF can specifically interact with a GPCR and modulate its G protein signaling specificity.

Introduction

G protein-coupled receptors (GPCRs) represent the largest group of cell surface proteins and transduce exogenous chemical and sensory stimuli (hormones, ions, lipids, neurotransmitters, light, and odors) into intracellular signals through activation of heterotrimeric G proteins. To couple specifically to distinct intracellular signaling pathways, GPCRs seem to interact with additional intracellular adaptor and signaling proteins and may form large protein complexes that tune the signals with respect to quality and quantity (Pierce et al., 2002).

To investigate the mechanisms of signaling specificity among different G proteins, we chose the model of the parathyroid hormone receptor (PTHR). The PTHR belongs to family B of GPCRs and is a main regulator of calcium homeostasis and bone metabolism and development (Potts, 2005). These effects are exerted through the activation of multiple signaling pathways. Binding of an agonist predominantly leads to stimulation of adenylyl cyclases through activation of G_s and stimulation of phospholipase Cβ through activation of G_q (Jüppner et al., 1991; Friedman, 2004; Vilardaga et al., 2011). Furthermore, the PTHR couples to $G_{i/o}$, which leads to adenylyl cyclase inhibition, and to $G_{12/13}$, which leads to phospholipase D and RhoA activation, and it can activate mitogen-activated protein kinases (Cole,

This work was supported by the Deutsche Forschungsgemeinschaft, Sonderforschungsbereich 487 "Regulatorische Membranproteine," Bayerische Forschungsstiftung (scholarship to A.E.N.), and the European Research Council [Advanced Grant "Towards the Quantal Nature of Receptor/cAMP Signals"].

Article, publication date, and citation information can be found at http://molpharm.aspetjournals.org.

http://dx.doi.org/10.1124/mol.112.078824.

[S] The online version of this article (available at http://molpharm.aspetjournals.org) contains supplemental material.

ABBREVIATIONS: GPCR, G protein-coupled receptor; α_{1B}-AR, α_{1B}-adrenergic receptor; CT, C-terminal domain; GEF, guanine nucleotide exchange factor; M-AChR, muscarinic acetylcholine receptor; NHERF, Na^+/H^+-exchanger regulatory factor; PDZ, postsynaptic density 95/*Drosophila* discs large/zona occludens; PLC, phospholipase C; PTH, parathyroid hormone; PTHR, parathyroid hormone receptor; DH, Dbl-homology; PH, pleckstrin-homology; PAGE, polyacrylamide gel electrophoresis; DMEM, Dulbecco's modified Eagle's medium; NP40, Nonidet P-40; dnNHERF, dominant-negative Na^+/H^+-exchanger regulatory factor 1(1–326); siRNA, small interfering RNA; HA, hemagglutinin; MERM, merlin/ezrin/radixin/moesin; IP, inositol phosphate; MBP, maltose-binding protein.

1999; Singh et al., 2005a,b; Mahon et al., 2006). These effects seem to be regulated in a tissue- and cell type-specific manner, which may explain the partially opposing physiological effects of PTH (Potts, 2005). Directed signaling to specific downstream pathways may be established through different arrangements of adaptor proteins within signaling complexes, which mediate signaling between pathway-specific receptor conformations and signaling pathway activation. It is unclear, however, how adaptation between different receptor conformations and differential pathway activation is achieved by adaptor proteins. For the PTHR, it has become increasingly clear that the C-terminal domain exhibits critical components for interactions with adaptor proteins that alter signaling and trafficking of the receptor (Vilardaga et al., 2001, 2002; Mahon et al., 2002, 2006; Klenk et al., 2010). Two members of the family of Na^+/H^+-exchanger regulatory factors (NHERFs) were shown to interact with intracellular parts of the PTHR (Mahon et al., 2002; Sneddon et al., 2003), and NHERFs thereby regulate trafficking and signaling of the PTHR (Wang et al., 2007, 2010; Wheeler et al., 2008). NHERF also propagates PTH-induced G_q/PLC activation and reduces adenylyl cyclase activity by stimulating inhibitory $G_{i/o}$ proteins (Mahon et al., 2002). The NHERF-PTHR complex is formed through a C-terminal PDZ binding cassette in the PTHR. The PTHR C-terminal domain serves to bind other adaptor and signaling proteins, such as β-arrestin and disheveled and heterotrimeric G proteins (Mahon et al., 2002, 2006; Vilardaga et al., 2002; Romero et al., 2010).

Other cytosolic and membrane-associated proteins have been implicated in the modulation of GPCR signaling specificity. Among them are several guanine nucleotide exchange factors (GEFs) for the Rho family of GTPases. These proteins catalyze the exchange of GDP for GTP in Rho GTPases and regulate various cellular functions. It is well known that several GPCRs are regulators of Rho proteins; of the >60 known RhoGEFs, four members have been determined to interact directly with α-subunits of heterotrimeric G proteins. p115RhoGEF and PDZRhoGEF both interact with $G\alpha_{12/13}$ (Mao et al., 1998; Fukuhara et al., 1999, 2001), leukemia-associated RhoGEF was found to mediate RhoA activation through both G_q- and $G_{12/13}$-coupled receptors, and p63RhoGEF is activated exclusively through $G_{q/11}$ (Fukuhara et al., 2000; Booden et al., 2002; Vogt et al., 2003; Lutz et al., 2005). Several lines of evidence indicate that Rho GTPases play an important role in bone remodeling. RhoA controls F-actin stress fiber formation and focal adhesions and thus has effects on osteoclast motility, podosome assembly, and bone metabolism (Chellaiah et al., 2000; Ory et al., 2008). It was shown in osteoblasts that expression of several osteogenic markers and cytokines, such as bone morphogenetic protein-2, osteocalcin, and interleukin-6, is regulated by RhoA, and this seems to be mediated through PTHR-dependent $G\alpha_{12/13}$ activation (Ohnaka et al., 2001; Radeff et al., 2004; Singh et al., 2005b). However, the exact molecular mechanisms of Rho activation as a signaling event downstream of the PTHR are not clear. In the present study, we have identified the RhoGEF vav2 as an adaptor protein for the PTHR and have shown that it regulates directed signaling of the receptor.

Materials and Methods

Materials. Human [$Nle^{8,18}$,Tyr^{34}]PTH(1-34) (referred to as PTH) was obtained from Peptide Specialty Laboratories GmbH (Heidelberg, Germany). Anti-HA-agarose (HA-7) and anti-c-myc-agarose were purchased from Sigma-Aldrich (St. Louis, MO). Monoclonal HA.11 (16B12) anti-HA antibody was purchased from Covance Research Products (Princeton, NJ). Anti-NHERF1 (EBP50) antibodies were obtained from Thermo Fisher Scientific (Waltham, MA), and anti-vav2 antibodies (EP1067Y) were purchased from Abcam plc (Cambridge, UK). Anti-$G\alpha_q$ polyclonal antibodies (C-19) were obtained from Santa Cruz Biotechnology Inc. (Santa Cruz, CA). Anti-His_6 and anti-myc (9B11) monoclonal antibodies were obtained from Cell Signaling Technology (Danvers, MA). Peroxidase-conjugated, anti-mouse and anti-rabbit secondary antibodies were obtained from Dianova (Hamburg, Germany). ON-TARGETplus small interfering RNA (siRNA) directed to human vav2 (si vav2) (GGAUGGAGCAGUUCGAGAU) and nontargeting siRNA (si Ctrl) (UGGUUUACAUGUCGACUAA) were obtained from Thermo Fisher Scientific. Amylose resin and enterokinase were obtained from New England Biolabs (Ipswich, MA). All other reagents were obtained from Sigma-Aldrich or Applichem (Darmstadt, Germany).

cDNA Constructs. Plasmids encoding HA-tagged human PTHR (HA-PTHR), HA-tagged, C-terminally truncated PTHR (HA-PTHR T480), and HA-tagged NHERF1 were described elsewhere (Dicker et al., 1999; Castro et al., 2002; Klenk et al., 2010). Dominant-negative $NHERF1^{1–326}$ (dnNHERF) was kindly provided by Peter A. Friedman (University of Pittsburgh School of Medicine, Pittsburgh, PA). Myc-vav2 and N- and C-terminally truncated myc-$vav2^{188–512}$ were kindly provided by Elisabeth Jeanclos (Rudolf Virchow Center, University of Würzburg, Würzburg, Germany). Human $G\alpha_q$, human muscarinic acetylcholine receptor (M-AChR) subtypes 1, 3, and 5, and human α_{1B}-adrenergic receptor (α_{1B}-AR) were purchased from Missouri S&T cDNA Resource Center (Rolla, MO). His_6-$G\alpha_s$ was kindly provided by Christiane Kleuß (Charité, University of Berlin, Berlin, Germany). The C-terminal domain of the PTHR (amino acids 463–593), with BamHI and SalI restriction sites at the 5′ and 3′ ends, respectively, was amplified through polymerase chain reaction with HA-PTHR as a template. After digestion with BamHI and SalI, the polymerase chain reaction product was subcloned into pMal-c3E (New England Biolabs) in-frame with the coding sequence for maltose-binding protein (MBP), which resulted in a MBP-PTHR-CT fusion construct. The sequences of all constructs were verified.

Proteomic Screen. The MBP-PTHR-CT fusion protein (described above) contained the PTHR-CT linked to MBP through an enterokinase cleavage site (Asp-Asp-Asp-Asp-Lys). MBP-PTHR-CT was recombinantly expressed in *Escherichia coli* BL21 and purified with affinity chromatography (amylose resin; New England Biolabs) and ion-exchange chromatography with an ÄKTA purifier system (Mono Q; GE Healthcare Technologies, Waukesha, WI). Two milligrams of the purified protein were immobilized on amylose resin and incubated for 14 to 16 h with cytosolic fractions of bovine kidney lysate (1 mg/ml) in 10 ml of buffer (20 mM Tris, 100 mM NaCl, 2 mM EDTA, 1 mM dithiothreitol, pH 7.5) supplemented with a mixture of protease inhibitors (10 μg/ml soybean trypsin inhibitor, 30 μg/ml benzamidine, 1 mg/ml leupeptin, and 100 μM phenylmethylsulfonyl fluoride). The resin was then washed with 100 column volumes of buffer (20 mM HEPES, 200 mM NaCl, 1 mM EDTA, 1% Triton X-100, pH 7.5), and the PTHR-CT and associated proteins were eluted through incubation with enterokinase (5 U/ml; New England Biolabs). Eluted proteins were subjected to SDS-PAGE and stained with Coomassie Blue. Twenty-three slices from each lane were digested with trypsin, as described previously (Shevchenko et al., 1996), and were analyzed through liquid chromatography-electrospray ionization-tandem mass spectrometry with an Orbitrap XL hybrid mass spectrometer (Thermo Fisher Scientific), under standard conditions. For determination of nonspecifically bound proteins,

control experiments were conducted separately by using MBP alone instead of MBP-PTHR-CT.

Cell Culture and Transfection. HEK 293 AD cells (referred to as HEK 293 cells) were maintained in Dulbecco's modified Eagle's medium (DMEM), and COS7 cells were maintained in 1:1 DMEM/Ham's F-12 medium. Tissue culture media were supplemented with 100 units/ml penicillin, 100 μg/ml streptomycin, and 10% (v/v) fetal calf serum. Cells were maintained at 37°C in a humidified atmosphere of 5% CO_2/95% air. For generation of stable cell lines, HEK 293 cells were transfected with HA-PTHR by using the calcium phosphate coprecipitation method. Forty-eight hours after transfection, the cells were selected for ~2 weeks in culture medium supplemented with 0.5 mg/ml G-418. Clonal cell lines were derived from limited dilution series and were screened for expression of the desired protein through Western blotting. Stable monoclonal cell lines were maintained in medium containing 0.2 mg/ml G-418.

For transient transfections, cells were plated 4 h before transfection. HEK 293 cells were transfected by using the calcium phosphate coprecipitation method, with 5 μg of plasmid encoding HA-PTHR, HA-PTHR T480, M-AChR subtypes, α_{1B}-AR, Gα_q, or His_6-Gα_s or 1 μg of plasmid encoding myc-vav2, HA-NHERF1, or dnNHERF per 10-cm culture dish. All transfection mixtures were adjusted to equal DNA amounts with empty vector. siRNAs were transfected at a concentration of 10 nM.

Coimmunoprecipitation of Vav2 and PTHR and Western Blotting. Cells were incubated with 5 μM latrunculin A at 37°C for 30 min. Cells were then stimulated with 500 nM PTH for 20 min. After stimulation, cells were scraped into and lysed in ice-cold NP40 lysis buffer [5 mM HEPES, pH 7.5, 150 mM NaCl, 1 mM EDTA, 10% (m/v) glycerol, 0.5% (m/v) NP40, 0.1% (m/v) dodecylmaltoside] supplemented with a mixture of protease inhibitors (as described above). Lysates were cleared through centrifugation at 20,000*g* for 30 min at 4°C, and supernatants were incubated for 2 h with anti-HA-agarose, anti-c-myc-agarose, or anti-myc antibodies bound to protein G-Sepharose (GE Healthcare Technologies). Precipitates were collected through gentle centrifugation and were washed three times with ice-cold NP40 lysis buffer. Proteins were eluted with SDS sample buffer, subjected to SDS-PAGE, and transferred to polyvinylidene difluoride membranes (Millipore Corp., Billerica, MA). The blots were incubated with primary antibodies as indicated, and bound antibody was visualized with secondary antibodies and ECL Plus Western blotting detection reagent (GE Healthcare Technologies), in accordance with the manufacturer's instructions.

Coimmunoprecipitation of Gα subunits was performed essentially as described above. For cell lysis, NP40/phosphate lysis buffer [5 mM sodium dihydrogen phosphate, pH 7.2, 150 mM NaCl, 1 mM EDTA, 10% (m/v) glycerol, 0.5% (m/v) NP40, 0.1% (m/v) dodecylmaltoside] supplemented with 5 mM $MgCl_2$, 10 μM GDP, 200 μM Na_3VO_4, a mixture of protease inhibitors (as described above), 30 μM $AlCl_3$, and 5 mM NaF was used.

Inositol Phosphate Accumulation. HEK 293 cells stably expressing HA-PTHR were transfected with siRNA directed against vav2, nontargeting siRNA, HA-NHERF1, or $NHERF1^{1-326}$, as indicated, and were grown in six-well plates. Cells were labeled for 16 h at 37°C with 1 μCi/ml [*myo*-2-^{3}H-(N)]inositol in inositol-free DMEM (MP Biomedicals, Solon, OH) containing 0.2% fetal calf serum. After labeling, cells were washed with 2 ml of HEPES buffer (20 mM HEPES, pH 7.3, 137 mM NaCl, 5 mM KCl, 1 mM $CaCl_2$, and 1 mM $MgCl_2$) per well and were incubated for 10 min in 1 ml per well of the same buffer supplemented with 10 mM LiCl. Cells were stimulated with PTH at the indicated concentrations for 60 min at 37°C. Stimulation was stopped with the addition of 120 μl of ice-cold 20% (v/v) $HClO_4$, and plates were rocked for 20 min on ice. Lysates were neutralized with 1 M KOH and centrifuged for 20 min at 20,000*g*. One milliliter of the supernatant was mixed with 2 ml of 5 mM Tris, pH 7.4, and applied to columns containing Dowex 1X8 ion-exchange resin (100–200 mesh). The resin was washed twice with 4 ml of double-distilled water, and [*myo*-2-^{3}H]inositol phosphates were eluted with the addition of 3 ml of 1 M HCl. Eluates were mixed with 15 ml of LumaSafe scintillation cocktail (PerkinElmer Life and Analytical Sciences, Waltham, MA), and β-emission of tritium was measured in a liquid scintillation counter.

cAMP Accumulation. HEK 293 cells stably expressing HA-PTHR were transfected with siRNA directed against vav2 or with nontargeting siRNA. The medium was aspirated, and 1 ml of HEPES buffer (20 mM HEPES, pH 7.3, 137 mM NaCl, 5 mM KCl, 1 mM $CaCl_2$, 1 mM $MgCl_2$) supplemented with 100 μM 3-isobutyl-1-methylxanthine was added to each well. Cells were stimulated with PTH at the indicated concentrations for 20 min at 37°C, and stimulation was stopped with the addition of 120 μl of ice-cold 20% (v/v) $HClO_4$ per well in a six-well plate. After 20 min on ice, lysates were neutralized with 1 M KOH and centrifuged for 20 min at 20,000*g*. cAMP levels were determined with a cAMP radioimmunoassay kit (Beckman Coulter, Fullerton, CA) and a Wallac 1480 automatic gamma counter (PerkinElmer Life and Analytical Sciences).

Data Processing. Statistical analyses and curve-fitting were performed by using Prism 4.0 (GraphPad Software Inc., San Diego, CA).

Results

Vav2 Binds to Intracellular Domains of the PTHR. The PTHR exhibits a large CT of ~130 amino acids, which is crucial for interactions with several adaptor and effector proteins that regulate receptor signaling (Vilardaga et al., 2001, 2002; Mahon et al., 2002, 2006). To identify novel PTHR-interacting proteins, we used a proteomic approach based on protein affinity and ion-exchange chromatography followed by mass spectrometry. Proteins associated with the PTHR were purified through affinity chromatography using the entire C-terminal domain (amino acids 464–593) of the receptor fused to MBP. For this, recombinantly expressed MBP-PTHR-CT was immobilized on amylose resin and cell lysates from bovine kidney were loaded on the columns. Bound proteins were eluted specifically through cleavage of an enterokinase site that had been inserted between MBP and the PTHR-CT. Eluted proteins were separated with SDS-PAGE and stained with Coomassie Blue, and 23 slices from the resulting gel were digested with trypsin and analyzed with liquid chromatography-electrospray ionization-tandem mass spectrometry. To exclude nonspecifically binding proteins, a control experiment using MBP alone, instead of MBP-PTHR-CT, was performed in parallel.

Through this screening, we identified three distinct peptides that corresponded to the guanine nucleotide exchange factor vav2 (Supplemental Fig. 1). To confirm the validity of these results and the specificity of the interaction, we performed coimmunoprecipitation experiments with PTHR and vav2 in a cellular system. For these experiments, myc-vav2 and full-length HA-PTHR were transiently expressed in HEK 293 cells. As a control, HA-PTHR lacking the intracellular C terminus (HA-PTHR T480) was used. Before precipitation of HA-tagged PTHR, cells were stimulated with PTH or were left unstimulated. As depicted in Fig. 1A, vav2 coprecipitated robustly with HA-PTHR, independent of stimulation with PTH. It is noteworthy that vav2 also coprecipitated with the truncated HA-PTHR T480; however, the interaction was significantly weaker, compared with full-length HA-PTHR. To confirm the interaction, overexpressed myc-vav2 was precipitated from HEK 293 cells, which led to specific coprecipitation of HA-PTHR (Fig. 1B). We also assessed the stoichiometry of the PTHR-vav2 interaction. To do

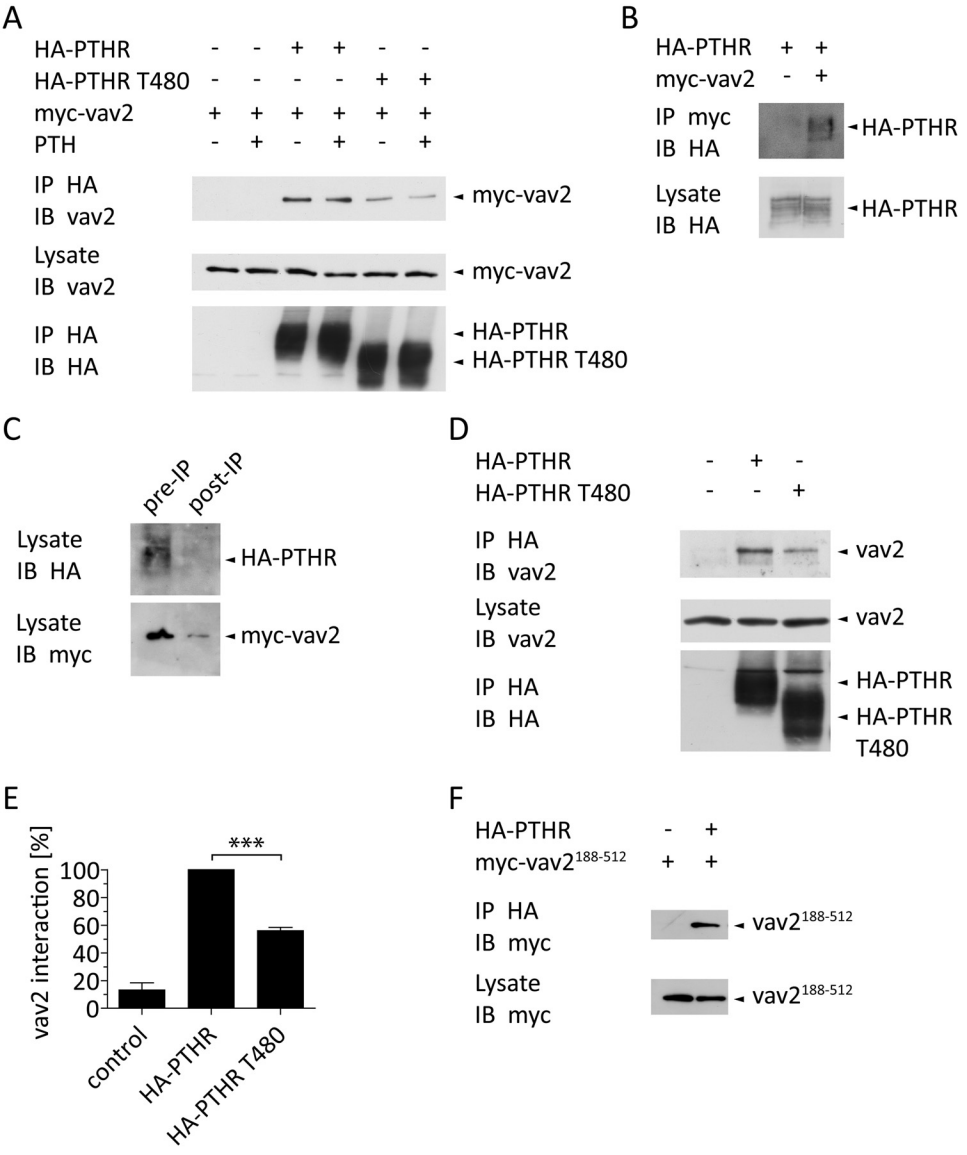

Fig. 1. Vav2 binds to intracellular domains of the PTHR. A, HEK 293 cells were transiently transfected with myc-vav2 and HA-PTHR or HA-PTHR T480, as indicated. Cells were stimulated with 500 nM PTH for 20 min, and HA-tagged receptors were immunoprecipitated with anti-HA affinity beads. Western blots of immunoprecipitates were probed for vav2 and HA, and cell lysates were probed for vav2. B, HEK 293 cells were transiently transfected with myc-vav2 and HA-PTHR, as indicated. Myc-vav2 was immunoprecipitated with anti-myc antibodies, and immunoprecipitates and cell lysates were probed for HA. C, HEK 293 cells grown on 10-cm plates were transiently transfected with cDNA coding for HA-PTHR (0.5 μg) and myc-vav2 (3 μg). Cells were lysed and myc-vav2 was quantitatively immunoprecipitated with anti-myc affinity beads. Western blots of corresponding amounts of lysate before and after vav2 precipitation were probed for HA and myc, as indicated. D, HEK 293 cells were transiently transfected with HA-PTHR or HA-PTHR T480, as indicated, and receptors were precipitated with anti-HA affinity beads. Western blots of cell lysates and immunoprecipitates were probed for vav2 and HA, as indicated. E, luminescence intensities obtained from antibodies bound to coprecipitated vav2 were measured and normalized. Data represent the mean ± S.E. (error bars) of five independent experiments. Statistical significance was determined with one-way analysis of variance. ***, $p < 0.001$. F, HEK 293 cells were transiently transfected with myc-vav2$^{188-512}$ and HA-PTHR, as indicated. HA-PTHR was immunoprecipitated with anti-HA affinity beads, and immunoprecipitates were probed for myc. IP, immunoprecipitation; IB, immunoblotting.

so, vav2 was immunoprecipitated quantitatively, and lysates before and after precipitation were probed for remaining PTHR and vav2. As shown in Fig. 1C, vav2 was almost completely precipitated from the lysate, and PTHR levels in the lysate were strongly reduced after immunoprecipitation, which indicated that the vast majority of the receptors were associated with vav2 under these conditions.

Unlike vav1, which is expressed exclusively in hematopoietic cells, vav2 is found in a wide range of tissues (Schuebel et al., 1996; Bustelo, 2000). Strong endogenous expression of vav2 is also found in kidney-derived HEK 293 cells. To test whether PTHR and vav2 coprecipitate at more-physiological expression levels, we tried to coimmunoprecipitate endogenous vav2 from HEK 293 cells transiently expressing HA-PTHR. Similar to overexpressed vav2, endogenous vav2 precipitated together with PTHR (Fig. 1D). Significantly weaker vav2 bands were detected in Western blots when PTHR T480 was immunoprecipitated. Densitometric analysis of the Western blots revealed 50% reduction of endogenous vav2 precipitated with PTHR T480, compared with PTHR (Fig. 1, D and E).

Vav proteins have complex structures, with multiple domains that promote specific interactions with other proteins. To delineate the part of vav2 that interacts with the PTHR, we used an N- and C-terminally truncated vav2 mutant, vav2$^{188–512}$. This mutant consists solely of a Dbl-homology (DH) domain, which exhibits RhoGEF activity, and a pleckstrin-homology (PH) domain, which is involved in subcellular targeting. HA-PTHR and myc-vav2$^{188–512}$ were transiently expressed in HEK 293 cells. Similar to the results with full-length vav2, myc-vav2$^{188–512}$ robustly precipitated with HA-PTHR (Fig. 1F).

Together with our results from the proteomic screening, these data indicate that vav2 is a novel PTHR-interacting protein. The DH and PH domains of vav2 were found to be sufficient for interactions with the C-terminal domain of the PTHR. Truncation of the C-terminal tail of the PTHR strongly reduced but did not completely abolish vav2 interactions, which suggests that other intracellular parts of the PTHR may serve as additional interfaces.

Vav2 Competes with PTHR for Coupling to Gα_q but Not to Gα_s. Several RhoA GEFs have been shown to scaffold

subunits of heterotrimeric G proteins and to modulate their activity (Mao et al., 1998; Fukuhara et al., 1999, 2000, 2001; Lutz et al., 2005). Therefore, we investigated whether vav2 might interfere with the cognate G protein signaling pathways of the PTHR. First we conducted coimmunoprecipitation experiments with the G protein subunits $G\alpha_q$ and $G\alpha_s$, which were transiently expressed together with myc-vav2 and HA-PTHR in HEK 293 cells. With stimulation with PTH and treatment with aluminum fluoride, G proteins were driven to and kept in the active state and myc-vav2 was immunoprecipitated. As shown in Fig. 2A, $G\alpha_s$ subunits did not coprecipitate with vav2 either in the presence or in the absence of PTHR. Next we performed coimmunoprecipitations with $G\alpha_q$ instead of $G\alpha_s$. In contrast to $G\alpha_s$, activated $G\alpha_q$ specifically coimmunoprecipitated with myc-vav2 (Fig. 2B). Remarkably, the amounts of coimmunoprecipitated $G\alpha_q$ were strongly increased in the absence of PTHR. This suggests that vav2 and PTHR compete for binding to activated $G\alpha_q$.

To address the question of whether $G\alpha_q$ activation is required to bind vav2, we activated $G\alpha_q$ either through PTH-induced PTHR activation or directly with aluminum fluoride before precipitation of myc-vav2. Nonactivated $G\alpha_q$ coprecipitated only weakly with myc-vav2, whereas stimulation with PTH led to a marked increase in the amount of coprecipitated $G\alpha_q$. Addition of aluminum fluoride had less-pronounced effects on the interaction between vav2 and $G\alpha_q$ (Fig. 2C). Next we asked whether vav2 might have an impact on PTHR coupling to $G\alpha_q$. We performed coimmunoprecipitation experiments with PTHR and $G\alpha_q$ in the presence of different vav2 expression levels. HA-PTHR and $G\alpha_q$ were transiently transfected in HEK 293 cells. Vav2 expression was specifically reduced with siRNA directed against endogenous vav2 or vav2 levels were increased through overexpression of myc-vav2. Cells were stimulated with PTH, and HA-PTHR was precipitated in the presence of aluminum fluoride. Precipitated proteins were separated with SDS-PAGE, and $G\alpha_q$ was detected through immunoblotting. Figure 2D shows that $G\alpha_q$ coimmunoprecipitated with activated PTHR and that the knockdown of endogenous vav2 did not detectably alter the amounts of coprecipitated $G\alpha_q$ and PTHR. With overexpression of myc-vav2, however, we found decreased interaction between $G\alpha_q$ and activated PTHR. These findings indicate that elevated vav2 levels can interfere with the binding of $G\alpha_q$ to the PTHR.

Vav2 Impairs PTH-Induced Inositol Phosphate Generation but Not cAMP Generation. As shown above, vav2 interacts with $G\alpha_q$ subunits of heterotrimeric G proteins and can modulate the binding of $G\alpha_q$ to the PTHR. Therefore, we asked whether vav2 might affect $G\alpha_q$-mediated PTHR signaling. For this purpose, a HEK 293 cell line stably expressing PTHR was generated, which allowed more-accurate investigation of PTHR signaling, compared with the use of cells transiently overexpressing PTHR. As in many other cell

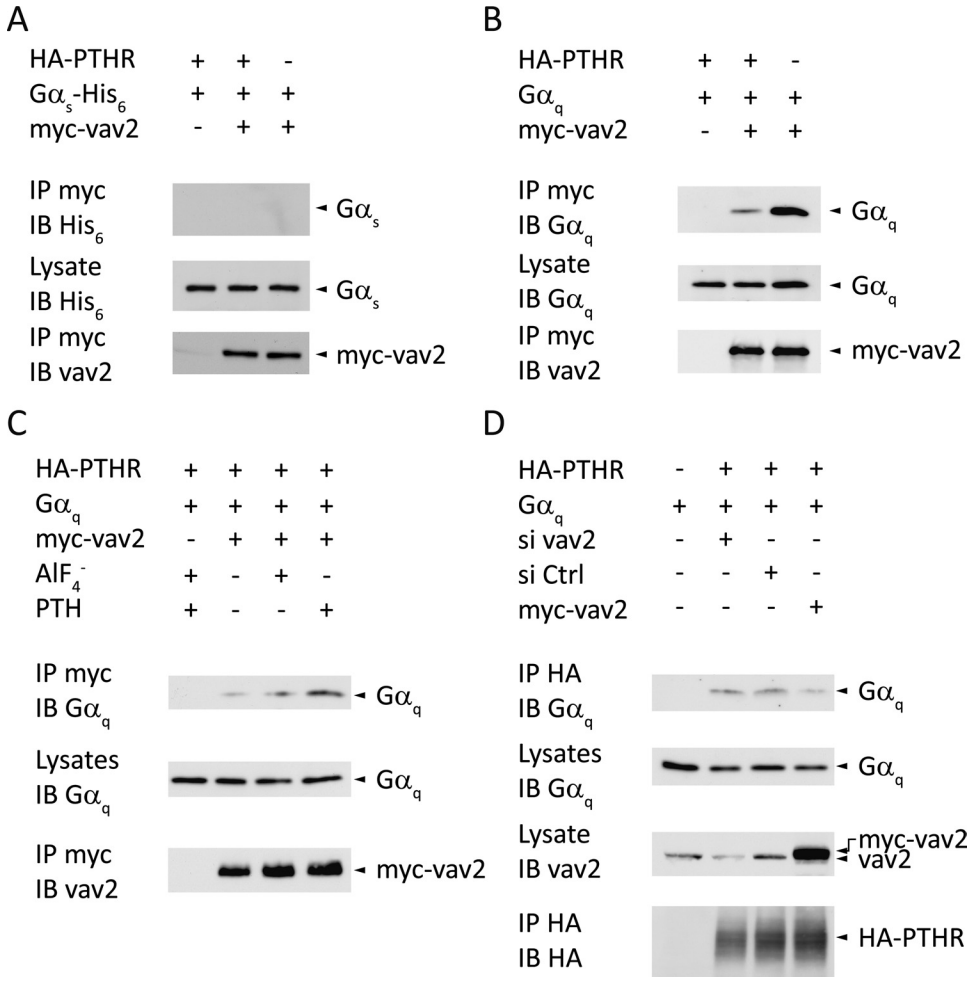

Fig. 2. Vav2 and PTHR compete for $G\alpha_q$ but not $G\alpha_s$. A and B, HEK 293 cells were transiently transfected with HA-PTHR, myc-vav2, and His_6-$G\alpha_s$ (A) or $G\alpha_q$ (B). Cells were stimulated with 500 nM PTH for 20 min, and myc-vav2 was immunoprecipitated with anti-myc antibodies in the presence of aluminum fluoride. Western blots of immunoprecipitates and cell lysates were probed for vav2 and His_6 (A) or $G\alpha_q$ (B), as indicated. C, HEK 293 cells were transiently transfected with HA-PTHR, $G\alpha_q$, and myc-vav2, as indicated. Cells were stimulated with 500 nM PTH for 20 min, as indicated. Myc-vav2 was immunoprecipitated with anti-myc antibodies in the presence or absence of aluminum fluoride. Western blots of cell lysates and immunoprecipitates were probed for $G\alpha_q$ and vav2. D, HEK 293 cells were transiently transfected with HA-PTHR, $G\alpha_q$, myc-vav2, siRNA against vav2 (si vav2), or nontargeting siRNA (si Ctrl), as indicated. Cells were stimulated with 500 nM PTH for 20 min, and HA-PTHR was immunoprecipitated in the presence of aluminum fluoride by using anti-HA affinity beads. Immunoprecipitates and cell lysates were assessed with immunoblotting for vav2, $G\alpha_q$, and HA. IP, immunoprecipitation; IB, immunoblotting.

types, vav2 is endogenously expressed at relatively high levels in HEK 293 cells. To ensure more-native conditions for cell signaling and to prevent nonspecific effects that might result from vav2 overexpression, we studied the effects of vav2 on PTHR signaling by reducing endogenous vav2 expression with siRNA. PTH-induced generation of [*myo*-2-^{3}H]inositol phosphates ([^{3}H]IPs) was markedly increased upon down-regulation of vav2 (with si vav2), compared with native vav2 expression levels (with si Ctrl) (Fig. 3A; Table 1). Basal [^{3}H]IP levels were not affected by siRNA transfections (si vav2 RNA: mean, −0.4%; 95% confidence interval: −9.0 to 8.2%; si Ctrl RNA: mean, 1.5%; 95% confidence interval: −9.3 to 12.3%).

In addition to monitoring the effects of vav2 on [^{3}H]IP accumulation, we studied the effects of vav2 depletion on cAMP accumulation. As described above, we used HEK 293 cells that stably expressed PTHR and were transfected with siRNA against vav2 or nontargeting siRNA. Cells were stimulated with PTH, and cAMP accumulation was measured in the presence of 3-isobutyl-1-methylxanthine. In contrast to G_q signaling, down-regulation of vav2 had no impact on G_s-mediated cAMP generation (Fig. 3B; Table 1). To ensure that vav2 knockdown did not impair PTHR expression levels, we controlled for PTHR expression in Western blots (Fig. 3C).

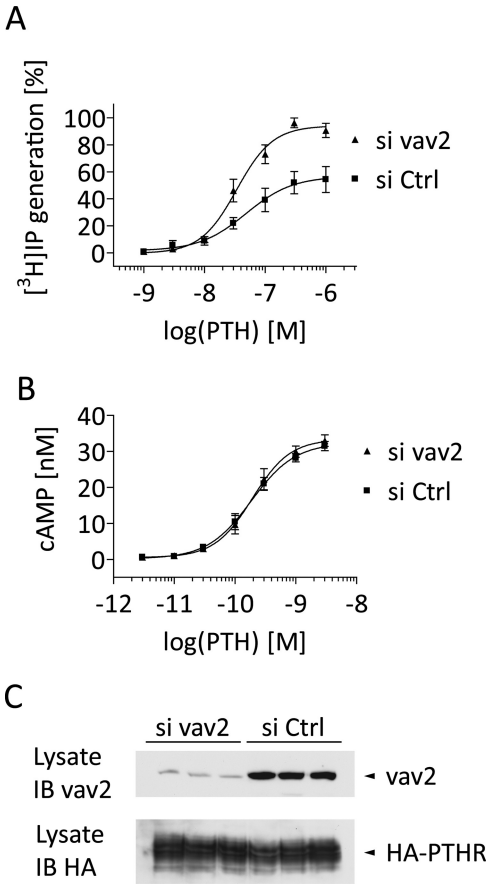

Fig. 3. Vav2 impairs PTH-induced IP generation but not cAMP generation. HEK 293 cells stably expressing HA-PTHR were transfected with siRNA against vav2 (si vav2) or nontargeting siRNA (si Ctrl). A, cells were incubated with [*myo*-2-^{3}H]inositol and 0.2% fetal calf serum for 16 h. Cells were stimulated for 60 min with the indicated concentrations of PTH, and [^{3}H]IP levels were quantified in a scintillation counter after chromatographic separation. Data represent the mean ± S.E. (error bars) of five individual experiments. B, HEK 293 cells were stimulated for 20 min with PTH at the indicated concentrations, and cAMP levels were quantified with a radioimmunoassay. Data of each experiment were normalized to minimal (0%) and maximal values (100%). The means ± S.E. (error bars) of five independent experiments are shown. C, the extent of vav2 knockdown and HA-PTHR expression levels were assessed through immunoblotting (IB) with anti-vav2 and anti-HA antibodies, respectively.

TABLE 1

Effects of vav2 knockdown on [^{3}H]IP and cAMP generation

The mean differences in [^{3}H]IP or cAMP generation induced by stimulation with 300 nM PTH were compared for vav2 knockdown and endogenous vav2 expression in HEK 293 cells with unpaired *t* tests. Data summarize results of five independent experiments.

	Difference, si Ctrl vs. si vav2		*p*
	Mean ± S.E.M.	95% C.I.	
[^{3}H]IP generation, %	44.3 ± 7.7	25.4 to 63.1	0.0012
cAMP generation, nM	1.5 ± 2.1	−3.3 to 6.2	0.49

C.I., confidence interval.

These findings support the experiments described above (Fig. 2, A and B) and suggest that vav2 specifically modulates the PTHR/Gα_q interaction but does not affect PTHR/Gα_s coupling. Our data indicate that vav2 is a negative regulator of PTH-induced PLC signaling, whereas PTH-induced adenylyl cyclase signaling remains unaffected.

Vav2 Specifically Inhibits G_q Signaling Evoked by PTHR Activation. Our findings that vav2 binds to both the PTHR and Gα_q and that it impairs signaling of the PTHR through G_q raises the question of whether the inhibition of signaling occurs primarily through the receptor or through Gα_q. Therefore, we investigated whether the inhibition of G_q signaling was specific for the PTHR or also occurred for other G_q-coupled receptors. For this investigation, HEK 293 cells were transfected with one of the following G_q-coupled receptors: PTHR, M_1-AChR, M_3-AChR, M_5-AChR, or α_{1B}-AR. Endogenous vav2 was depleted with cotransfection of a siRNA against vav2. Receptors were stimulated with full agonists (PTHR, 300 nM PTH; M_1-AChR, M_3-AChR, and M_5-AChR, 100 μM carbachol; α_{1B}-AR, 10 μM norepinephrine), and [^{3}H]IP accumulation was measured. For each receptor, a robust >10-fold increase in [^{3}H]IP levels was measured after agonist addition (data not shown). Similar to the findings described above, vav2 knockdown resulted in a ~60% increase in IP accumulation after activation of the PTHR, compared with the use of control siRNA. A difference in IP accumulation in vav2-depleted cells versus control cells was observed for none of the other G_q-coupled receptors (Fig. 4). This clearly indicates that vav2 specifically inhibits PTHR-mediated G_q signaling and exerts its inhibitory effect primarily at the receptor level.

The NHERF1 MERM Domain Is Required for Increased IP Generation with Vav2 Knockdown. Our data provide evidence that direct or indirect interactions of vav2 with PTHR and Gα_q specifically lead to inhibition of PLC-mediated signaling. Similar to our findings for vav2, NHERF1 and NHERF2 were shown previously to interact with PTHR in a stimulation-independent manner. In contrast to vav2, however, NHERF1 and NHERF2 propagate PLC signaling of the PTHR by scaffolding PLCβ (Mahon et al., 2002; Klenk et al., 2010). We and others have demonstrated that NHERF1 also acts as a scaffold for β-arrestin at the PTHR-CT, which leads to accelerated receptor desensitization (Mahon and Segre, 2004; Klenk et al., 2010). Therefore, we addressed the question of whether vav2 would interfere

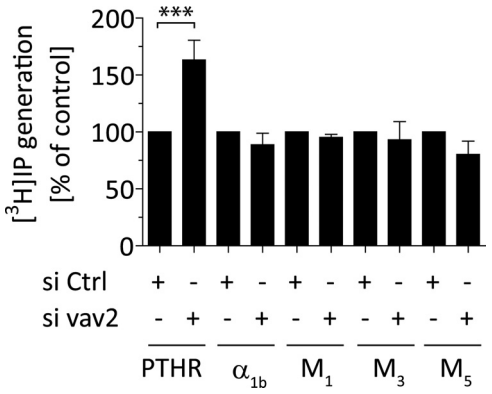

Fig. 4. Vav2 specifically attenuates PTHR-mediated IP generation. HEK 293 cells transiently expressing the indicated GPCRs were transfected with siRNA against vav2 (si vav2) or nontargeting siRNA (si Ctrl). Cells were incubated with [*myo*-2-^{3}H]inositol and 0.2% fetal calf serum for 16 h. Then cells were stimulated with 300 nM PTH (PTHR), 100 μM carbachol (M_1-AChR, M_3-AChR, and M_5-AChR), or 10 μM norepinephrine (α_{1B}-AR) for 60 min, and [^{3}H]IP levels were quantified as in Fig. 3. Agonist-induced stimulation was >10-fold for all receptors. Data were normalized to the control group values for every receptor and are given as the mean ± S.E. (error bars) of four independent experiments. One-way analysis of variance and Bonferroni's multiple-comparison post hoc test determined statistical significance; ***, $p < 0.001$.

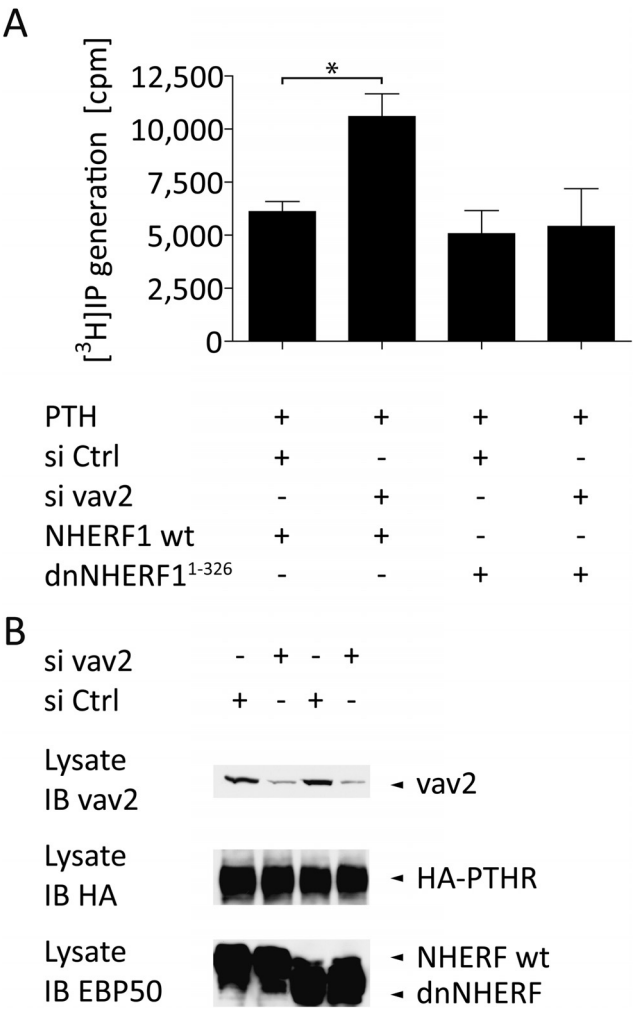

Fig. 5. The NHERF1 MERM domain is required for increased IP generation upon vav2-knockdown. HEK 293 cells stably expressing HA-PTHR were transfected with siRNA against vav2 (si vav2) or nontargeting siRNA (si Ctrl), as well as NHERF1 wild-type (NHERF wt) or dnNHERF, as indicated. A, cells were incubated with [*myo*-2-^{3}H]inositol and 0.2% fetal calf serum for 16 h. Cells were stimulated with 300 nM PTH for 60 min, and [^{3}H]IP levels were quantified as in Fig. 3. Unstimulated (i.e., without PTH) values were 172 ± 26 cpm under all conditions. Data represent the mean ± S.E. (error bars) of four independent experiments. Statistical significance was determined with one-way analysis of variance followed by Bonferroni's multiple-comparison post hoc test. *, $p < 0.05$. B, vav2 knockdown and expression levels of HA-PTHR and NHERF1 proteins were assessed through immunoblotting (IB) with anti-vav2, anti-HA, and anti-EBP50 antibodies, respectively.

with the effects of NHERF1 on PTH-induced IP accumulation. An important prerequisite for the scaffolding function of NHERF1 is its C-terminal MERM binding domain, which connects the signaling complexes to the cytoskeleton (Voltz et al., 2001); therefore, HA-PTHR-expressing HEK 293 cells were transfected either with NHERF1 or with the dnNHERF mutant lacking the MERM domain (Weinman et al., 2001; Li et al., 2002). In addition, cells were transfected with siRNA oligonucleotides directed against vav2 or with nontargeting siRNAs. Subsequently, cells were stimulated with 300 nM PTH for 60 min, and IP generation was measured. Similar to the findings shown in Fig. 3A, we observed approximately 2-fold increased IP levels after knockdown of vav2 in NHERF-expressing cells, compared with cells expressing vav2 (Fig. 5A). dnNHERF completely abolished the effect of vav2 knockdown on IP generation, with IP generation at equally low levels, compared with vav2-expressing cells (Fig. 5A). The efficacy of vav2 knockdown and expression levels of PTHR and NHERF were controlled in Western blots (Fig. 5B). These data suggest that vav2 interferes with the NHERF1-facilitated activation of PLC through the PTHR.

Discussion

In recent years, it has become increasingly clear that signaling processes from the plasma membrane to intracellular compartments are highly regulated spatially and temporally (Lohse et al., 2012). Especially for receptors that can activate as many diverse G protein-initiated signaling pathways as the PTHR, fine-tuned regulation of signaling seems necessary for the exertion of specific cellular effects. Such regulation can be provided by diverse scaffold and adaptor proteins that can specifically interact with receptors, G proteins, and/or effectors, forming dynamic signaling complexes in the proximity of the receptor. In this study, we set out to identify proteins that interact with and regulate the signaling properties of the PTHR. A biochemical interaction assay using the immobilized C-terminal domain of the PTHR combined with mass spectrometric analysis allowed us to screen native tissues, such as kidney, that endogenously express PTHR. On the basis of this initial screening, we identified the RhoGEF vav2 as a PTHR-interacting protein. PTHR interacted strongly with vav2 in cells, and the majority of receptors were associated with vav2 in our model, which strongly suggests a functional role for the interaction. Although the interaction screening was performed with the PTHR-CT, a truncated version of the PTHR that lacked most of the C-terminal tail (PTHR T480) was still able to bind vav2, albeit weakly. This finding suggests that vav2 may make additional contacts with the PTHR, presumably between amino acids 463 and 480 within the C-terminal tail or at intracellular loops. Because vav2 binding to PTHR T480 was strongly impaired, compared with binding to the full-length PTHR, we conclude

that the C terminus of the PTHR provides the most important binding site for vav2. Additional mapping of the PTHR binding interface was not possible, because truncation of the PTHR upstream of position 480 resulted in nonfunctional receptor mutants (data not shown).

The major PTHR interaction interface in vav2 most likely includes the tandem DH and PH domains, as indicated by pulldown experiments with the DH/PH domain-containing vav2 truncant vav2$^{188-512}$. It is interesting to note that the activation of PTHR by PTH and the subsequent signaling and trafficking events did not detectably affect the interaction of vav2 with the receptor. Together, our protein-protein interaction data show that vav2, a guanine nucleotide exchange factor for small GTPases, can associate with the heterotrimeric G protein-coupled PTHR.

These results are in line with findings showing that several RhoGEFs are able to interact directly with heterotrimeric G proteins (Fukuhara et al., 1999, 2000; Lutz et al., 2005, 2007). Most of these RhoGEFs harbor a regulator of G protein signaling homology domain, which is required for interaction with activated G proteins of the $G\alpha_{12}$ subfamily (Mao et al., 1998; Fukuhara et al., 1999, 2000). In contrast, p63RhoGEF does not contain regulator of G protein signaling domains and interacts with $G\alpha_q$ through its PH and DH domains (Lutz et al., 2007).

We next addressed the question of whether the vav2/PTHR interaction has relevance for G protein-mediated PTHR signaling. We found that vav2 preferentially binds to activated $G\alpha_q$ but not to $G\alpha_s$. The amount of activated $G\alpha_q$ bound to vav2 was dramatically decreased with coexpression of PTHR, and vice versa, which indicates that vav2 may function as a switch that modulates G_q coupling to the PTHR. Because vav2 most likely interacts with the C-terminal tail and intracellular loops of PTHR, it is conceivable that this interaction sterically interferes with $G\alpha_q$ coupling. Studies on the G protein-binding interface for PTHR suggest that critical components for G protein coupling are present at residues 468 to 491 of the C-terminal tail of the PTHR (Mahon et al., 2006). Other studies on PTHR signaling with the C-terminally truncated PTHR T480 revealed G_q-mediated IP generation to be even more efficient with the truncated T480 mutant (Dicker et al., 1999; Castro et al., 2002). These data suggest that C-terminal residues between 468 and 480 may play an important role in PTHR coupling to $G\alpha_q$. As mentioned above, vav2 may exhibit binding capacities for the PTHR upstream of residue 480; therefore, vav2 and G proteins may share a common binding interface on PTHR.

Our data revealed that vav2 modulated $G\alpha_q$ coupling to the PTHR. We next investigated whether this competitive action would affect PTH-induced generation of second messengers. We observed that vav2 negatively regulated PTH-induced IP generation, inasmuch as vav2 knockdown increased IP accumulation. In contrast, vav2 overexpression resulted in reduced IP levels after PTHR activation, which corroborated our findings (data not shown). cAMP accumulation was not affected by vav2 knockdown. These findings emphasize that vav2 specifically interferes with $G\alpha_q$ coupling to the PTHR. This interference with G_q signaling by vav2 was specific for the PTHR, because signaling from other G_q-coupled receptors was not altered by vav2. It seems likely that the interaction of vav2 with PTHR-CT is the key feature in its ability to block G_q signaling from the receptor.

In this regard, vav2 and NHERF display remarkable similarities; both proteins constitutively interact with the PTHR. NHERF positively regulates G_q signaling, whereas the present findings indicate that vav2 negatively regulates G_q signaling. The two PDZ domains of NHERF were shown to direct PLCs and PTHR to signaling complexes for effective signaling (Mahon and Segre, 2004; Sun and Mierke, 2005). Furthermore, evidence that PTHR signaling and trafficking are directed by NHERF-assembled microdomains was reported (Mahon and Segre, 2004; Ardura et al., 2011). These microdomains are assembled by NHERF proteins, which link signaling complexes to the cytoskeleton through the MERM domain. Our experiments indicated that overexpression of dnNHERF, which is lacking the MERM domain, did not affect PTH-induced IP generation per se. However, disruption of the NHERF-actin interaction completely abolished the increase in G_q signaling provoked by vav2 depletion. From this finding, we conclude that vav2 may constitute a specific counterpart to NHERF-directed PLC signaling.

The results from this work provide evidence for vav2 being a negative regulator of PTHR-G_q signaling. The physiological roles of this novel interaction remain to be determined. It is noteworthy that several lines of evidence indicate that vav proteins may play a role in bone metabolism in vivo. In one study, homozygote vav3-knockout mice exhibited increased bone mass induced by PTH and were less sensitive to bone resorption induced by PTH or receptor activator of nuclear factor κB ligand (Faccio et al., 2005). Although this study did not reveal an effect in vav2-knockout mice, distinct expression patterns for vav subtypes and differences in the phenotypes of selective vav-knockout mice raise questions regarding the hypothesis of complete functional redundancy of vav isoforms. However, a phenotype for homozygous vav2-knockout mice has not been reported (Turner and Billadeau, 2002). Recent studies indicated that G_q signaling, which leads to IP generation, can inhibit osteoanabolic effects of PTH (Ogata et al., 2011). The vav2-dependent modulation of PTH-induced G_q signaling may be relevant for this mechanism, and the interaction of vav2 and PTHR described here may contribute to our understanding of the physiological regulation of PTH-mediated signaling events.

In summary, our data show that vav2, which is known to function as a nucleotide exchange factor for Rho GTPases, can interact specifically with a GPCR and control its signaling specificity by directing PTHR signaling away from G_q. These results reveal another element of the complex network that controls intracellular signaling.

Acknowledgments

We thank Michaela Hoffmann for technical assistance and Dr. Elisabeth Jeanclos for providing vav2 constructs.

Authorship Contributions

Participated in research design: Gohla, Lohse, and Klenk.
Conducted experiments: Emami-Nemini.
Performed data analysis: Emami-Nemini, Urlaub, and Klenk.
Wrote or contributed to the writing of the manuscript: Emami-Nemini, Gohla, Urlaub, Lohse, and Klenk.

References

Ardura JA, Wang B, Watkins SC, Vilardaga JP, and Friedman PA (2011) Dynamic Na^+-H^+ exchanger regulatory factor-1 association and dissociation regulate para-

thyroid hormone receptor trafficking at membrane microdomains. *J Biol Chem* **286:**35020–35029.
Booden MA, Siderovski DP, and Der CJ (2002) Leukemia-associated Rho guanine nucleotide exchange factor promotes Gαq-coupled activation of RhoA. *Mol Cell Biol* **22:**4053–4061.
Bustelo XR (2000) Regulatory and signaling properties of the Vav family. *Mol Cell Biol* **20:**1461–1477.
Castro M, Dicker F, Vilardaga JP, Krasel C, Bernhardt M, and Lohse MJ (2002) Dual regulation of the parathyroid hormone (PTH)/PTH-related peptide receptor signaling by protein kinase C and beta-arrestins. *Endocrinology* **143:**3854–3865.
Chellaiah MA, Soga N, Swanson S, McAllister S, Alvarez U, Wang D, Dowdy SF, and Hruska KA (2000) Rho-A is critical for osteoclast podosome organization, motility, and bone resorption. *J Biol Chem* **275:**11993–12002.
Cole JA (1999) Parathyroid hormone activates mitogen-activated protein kinase in opossum kidney cells. *Endocrinology* **140:**5771–5779.
Dicker F, Quitterer U, Winstel R, Honold K, and Lohse MJ (1999) Phosphorylation-independent inhibition of parathyroid hormone receptor signaling by G protein-coupled receptor kinases. *Proc Natl Acad Sci USA* **96:**5476–5481.
Faccio R, Teitelbaum SL, Fujikawa K, Chappel J, Zallone A, Tybulewicz VL, Ross FP, and Swat W (2005) Vav3 regulates osteoclast function and bone mass. *Nat Med* **11:**284–290.
Friedman PA (2004) PTH revisited. *Kidney Int Suppl* **(91):**S13–S19.
Fukuhara S, Chikumi H, and Gutkind JS (2000) Leukemia-associated Rho guanine nucleotide exchange factor (LARG) links heterotrimeric G proteins of the G_{12} family to Rho. *FEBS Lett* **485:**183–188.
Fukuhara S, Chikumi H, and Gutkind JS (2001) RGS-containing RhoGEFs: the missing link between transforming G proteins and Rho? *Oncogene* **20:**1661–1668.
Fukuhara S, Murga C, Zohar M, Igishi T, and Gutkind JS (1999) A novel PDZ domain containing guanine nucleotide exchange factor links heterotrimeric G proteins to Rho. *J Biol Chem* **274:**5868–5879.
Jüppner H, Abou-Samra AB, Freeman M, Kong XF, Schipani E, Richards J, Kolakowski LF Jr, Hock J, Potts JT Jr, and Kronenberg HM (1991) A G protein-linked receptor for parathyroid hormone and parathyroid hormone-related peptide. *Science* **254:**1024–1026.
Klenk C, Vetter T, Zürn A, Vilardaga JP, Friedman PA, Wang B, and Lohse MJ (2010) Formation of a ternary complex among NHERF1, β-arrestin, and parathyroid hormone receptor. *J Biol Chem* **285:**30355–30362.
Li JG, Chen C, and Liu-Chen LY (2002) Ezrin-radixin-moesin-binding phosphoprotein-50/Na^+/H^+ exchanger regulatory factor (EBP50/NHERF) blocks U50,488H-induced down-regulation of the human kappa opioid receptor by enhancing its recycling rate. *J Biol Chem* **277:**27545–27552.
Lohse MJ, Nuber S, and Hoffmann C (2012) Fluorescence/bioluminescence resonance energy transfer techniques to study G-protein-coupled receptor activation and signaling. *Pharmacol Rev* **64:**299–336.
Lutz S, Freichel-Blomquist A, Yang Y, Rümenapp U, Jakobs KH, Schmidt M, and Wieland T (2005) The guanine nucleotide exchange factor p63RhoGEF, a specific link between $G_{q/11}$-coupled receptor signaling and RhoA. *J Biol Chem* **280:**11134–11139.
Lutz S, Shankaranarayanan A, Coco C, Ridilla M, Nance MR, Vettel C, Baltus D, Evelyn CR, Neubig RR, Wieland T, et al. (2007) Structure of Gαq-p63RhoGEF-RhoA complex reveals a pathway for the activation of RhoA by GPCRs. *Science* **318:**1923–1927.
Mahon MJ, Bonacci TM, Divieti P, and Smrcka AV (2006) A docking site for G protein βγ subunits on the parathyroid hormone 1 receptor supports signaling through multiple pathways. *Mol Endocrinol* **20:**136–146.
Mahon MJ, Donowitz M, Yun CC, and Segre GV (2002) Na^+/H^+ exchanger regulatory factor 2 directs parathyroid hormone 1 receptor signalling. *Nature* **417:**858–861.
Mahon MJ and Segre GV (2004) Stimulation by parathyroid hormone of a NHERF-1-assembled complex consisting of the parathyroid hormone I receptor, phospholipase Cβ, and actin increases intracellular calcium in opossum kidney cells. *J Biol Chem* 279:23550–23558.
Mao J, Yuan H, Xie W, and Wu D (1998) Guanine nucleotide exchange factor GEF115 specifically mediates activation of Rho and serum response factor by the G protein alpha subunit Gα13. *Proc Natl Acad Sci USA* 95:12973–12976.
Ogata N, Shinoda Y, Wettschureck N, Offermanns S, Takeda S, Nakamura K, Segre GV, Chung UI, and Kawaguchi H (2011) Gαq signal in osteoblasts is inhibitory to the osteoanabolic action of parathyroid hormone. *J Biol Chem* **286:**13733–13740.
Ohnaka K, Shimoda S, Nawata H, Shimokawa H, Kaibuchi K, Iwamoto Y, and Takayanagi R (2001) Pitavastatin enhanced BMP-2 and osteocalcin expression by inhibition of Rho-associated kinase in human osteoblasts. *Biochem Biophys Res Commun* **287:**337–342.
Ory S, Brazier H, Pawlak G, and Blangy A (2008) Rho GTPases in osteoclasts: orchestrators of podosome arrangement. *Eur J Cell Biol* **87:**469–477.
Pierce KL, Premont RT, and Lefkowitz RJ (2002) Seven-transmembrane receptors. *Nat Rev Mol Cell Biol* **3:**639–650.
Potts JT (2005) Parathyroid hormone: past and present. *J Endocrinol* **187:**311–325.
Radeff JM, Nagy Z, and Stern PH (2004) Rho and Rho kinase are involved in parathyroid hormone-stimulated protein kinase C alpha translocation and IL-6 promoter activity in osteoblastic cells. *J Bone Miner Res* **19:**1882–1891.
Romero G, Sneddon WB, Yang Y, Wheeler D, Blair HC, and Friedman PA (2010) Parathyroid hormone receptor directly interacts with dishevelled to regulate beta-catenin signaling and osteoclastogenesis. *J Biol Chem* **285:**14756–14763.
Schuebel KE, Bustelo XR, Nielsen DA, Song BJ, Barbacid M, Goldman D, and Lee IJ (1996) Isolation and characterization of murine vav2, a member of the vav family of proto-oncogenes. *Oncogene* **13:**363–371.
Shevchenko A, Wilm M, Vorm O, and Mann M (1996) Mass spectrometric sequencing of proteins silver-stained polyacrylamide gels. *Anal Chem* **68:**850–858.
Singh AT, Frohman MA, and Stern PH (2005a) Parathyroid hormone stimulates phosphatidylethanolamine hydrolysis by phospholipase D in osteoblastic cells. *Lipids* **40:**1135–1140.
Singh AT, Gilchrist A, Voyno-Yasenetskaya T, Radeff-Huang JM, and Stern PH (2005b) Gα12/Gα13 subunits of heterotrimeric G proteins mediate parathyroid hormone activation of phospholipase D in UMR-106 osteoblastic cells. *Endocrinology* **146:**2171–2175.
Sneddon WB, Syme CA, Bisello A, Magyar CE, Rochdi MD, Parent JL, Weinman EJ, Abou-Samra AB, and Friedman PA (2003) Activation-independent parathyroid hormone receptor internalization is regulated by NHERF1 (EBP50). *J Biol Chem* **278:**43787–43796.
Sun C and Mierke DF (2005) Characterization of interactions of Na^+/H^+ exchanger regulatory factor-1 with the parathyroid hormone receptor and phospholipase C. *J Pept Res* **65:**411–417.
Turner M and Billadeau DD (2002) VAV proteins as signal integrators for multi-subunit immune-recognition receptors. *Nat Rev Immunol* **2:**476–486.
Vilardaga JP, Frank M, Krasel C, Dees C, Nissenson RA, and Lohse MJ (2001) Differential conformational requirements for activation of G proteins and the regulatory proteins arrestin and G protein-coupled receptor kinase in the G protein-coupled receptor for parathyroid hormone (PTH)/PTH-related protein. *J Biol Chem* **276:**33435–33443.
Vilardaga JP, Krasel C, Chauvin S, Bambino T, Lohse MJ, and Nissenson RA (2002) Internalization determinants of the parathyroid hormone receptor differentially regulate beta-arrestin/receptor association. *J Biol Chem* **277:**8121–8129.
Vilardaga JP, Romero G, Friedman PA, and Gardella TJ (2011) Molecular basis of parathyroid hormone receptor signaling and trafficking: a family B GPCR paradigm. *Cell Mol Life Sci* **68:**1–13.
Vogt S, Grosse R, Schultz G, and Offermanns S (2003) Receptor-dependent RhoA activation in G_{12}/G_{13}-deficient cells: genetic evidence for an involvement of G_q/G_{11}. *J Biol Chem* **278:**28743–28749.
Voltz JW, Weinman EJ, and Shenolikar S (2001) Expanding the role of NHERF, a PDZ-domain containing protein adapter, to growth regulation. *Oncogene* **20:**6309–6314.
Wang B, Ardura JA, Romero G, Yang Y, Hall RA, and Friedman PA (2010) Na/H exchanger regulatory factors control parathyroid hormone receptor signaling by facilitating differential activation of Gα protein subunits. *J Biol Chem* **285:**26976–26986.
Wang B, Bisello A, Yang Y, Romero GG, and Friedman PA (2007) NHERF1 regulates parathyroid hormone receptor membrane retention without affecting recycling. *J Biol Chem* **282:**36214–36222.
Weinman EJ, Evangelista CM, Steplock D, Liu MZ, Shenolikar S, and Bernardo A (2001) Essential role for NHERF in cAMP-mediated inhibition of the Na^+-HCO_3^- co-transporter in BSC-1 cells. *J Biol Chem* **276:**42339–42346.
Wheeler D, Garrido JL, Bisello A, Kim YK, Friedman PA, and Romero G (2008) Regulation of parathyroid hormone type 1 receptor dynamics, traffic, and signaling by the Na^+/H^+ exchanger regulatory factor-1 in rat osteosarcoma ROS 17/2.8 cells. *Mol Endocrinol* **22:**1163–1170.

Address correspondence to: Dr. Martin J. Lohse, Institute of Pharmacology and Toxicology, Rudolf Virchow Center, University of Würzburg, Versbacher Straße 9, D-97078 Würzburg, Germany. E-mail: lohse@toxi.uni-wuerzburg.de